Dissociative recombination dynamics of the ozone cation

V. Zhaunerchyk,* W. D. Geppert, F. Österdahl, M. Larsson, and R. D. Thomas
Department of Physics, Albanova University Centre, Stockholm University, SE-106 91 Stockholm, Sweden

E. Bahati, M. E. Bannister, M. R. Fogle, and C. R. Vane
Physics Division, Oak Ridge National Laboratory, P.O. Box 2008, Oak Ridge, Tennessee, 37831-6377, USA
(Received 31 October 2007; published 6 February 2008)

The dissociative recombination of the ozone cation has been studied at the heavy-ion storage ring CRYRING. The total cross section and branching fractions have been measured. The cross section from ≈ 0 eV to 0.2 eV follows a nearly E^{-1} dependence, which was theoretically predicted to be a characteristic of the direct dissociative recombination mechanism. The thermal rate coefficient has been deduced from the cross section to be $7.37 \times 10^{-7}(T/300)^{-0.55}$ cm^3 s^{-1}. The branching fraction analysis carried out at ≈ 0 eV interaction energy has shown a strong propensity (94%) to dissociate through the three-body channel. Due to the overwhelming dominance of this channel it has been investigated in more detail. Of the six energetically available three-body pathways only three are significantly populated, such that the production of $O(^1S)$ is highly unfavored and all atomic oxygen fragments are predominantly formed in ^3P and ^1D states. Analysis of the breakup geometries has been performed by means of the Dalitz plot. It is observed that the molecules dissociating through the $O(^3P)+O(^3P)+O(^3P)$ and $O(^3P)+O(^3P)+O(^1D)$ channels have an open linear geometry where the cleavage of two valence bonds occurs preferentially in unison, while the $O(^3P)+O(^1D)+O(^1D)$ breakup might proceed partly through a sequential mechanism.

DOI: 10.1103/PhysRevA.77.022704 PACS number(s): 34.80.Ht

I. INTRODUCTION

In spite of the low concentration of ozone in the stratosphere (10 ppm peak concentration) it plays a crucial role in the absorption of biologically harmful solar ultraviolet radiation in the range 240–290 nm. Many experimental and theoretical studies have been devoted to neutral ozone and its atmospherically relevant chemical reactions, while the cation has received much less attention. One of the possible reactions to form the ozone cation involves neutral and ionized oxygen molecules [1,2]

$$O_2^+(^4\Pi, v \geq 5) + O_2(^3\Sigma_g^-) \rightarrow O_3^+ + O. \quad (1)$$

In oxygen containing plasmas O_3^+ can efficiently react with electrons. Among the different molecular ion-electron interaction reactions dissociative recombination (DR) is of great interest because of its importance for the terrestrial atmosphere [3] and astrophysical environments [4].

DR is a process in which a molecular ion recombines with an electron and subsequently dissociates into neutral fragments. Since DR is a binary collision process and very efficient at low interaction energies, it is the most dominant neutralizing mechanism in low-pressure and low-temperature plasmas. Due to the high exothermicity of the DR process (usually several eV) it can lead to the formation of both translationally hot and internally excited products. Knowledge about the internal states of the products is very important. DR of the ozone cation can create atomic oxygen in several different electronically excited states (Fig. 1). Atomic oxygen in the first excited state (^1D) is more reactive than the ground state species and is responsible for the red aurora and airglow when the atom relaxes back to the ground state, while the second excited state (^1S) is a source for the green aurora and airglow [5]. Investigations at storage rings of the fragmentation into the different excited product states resulting from the DR reaction has been possible due to the development and use of a position-sensitive imaging detector [6].

In the DR of polyatomic molecular ions different sets of neutral fragments can be formed. Before the introduction of the storage rings which enabled highly accurate measurements of the DR branching fractions to be performed, several

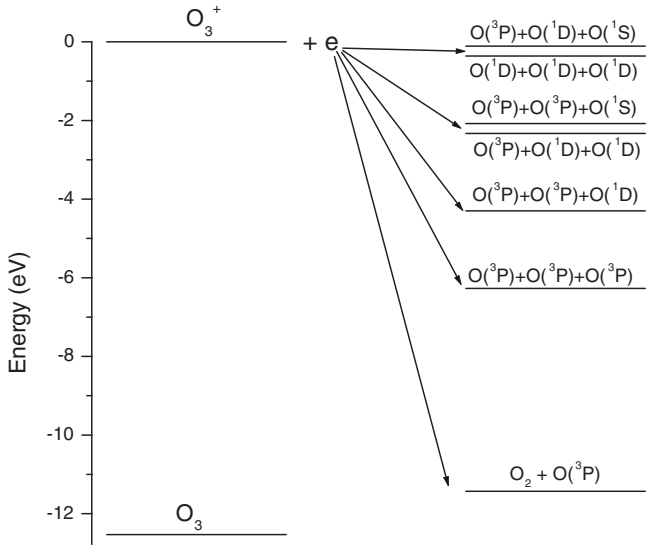

FIG. 1. The energetics in DR of O_3^+ at 0 eV interaction energy assuming that the molecules are in their ground states. Zero energy corresponds to the ground state of O_3^+.

*Author to whom correspondence should be addressed: vz@physto.se

models had been utilized to predict the fragmentation [7–10]. One of them, which was extensively applied [11], was created by Bates in 1986 [9,10]. This model argues that DR involves the least rearrangement of valence bonds. However, a tendency for DR of valence triatomic dihydrides (XH_2^+) to proceed through three-body breakup has experimentally been observed to constitute about 60–80 % of the total reactivity [12–16]. The three-body channel as a main route for DR has also been observed for several other polyatomic ions [17,18]. Recently, Larsson and Thomas reviewed the dynamics of the three-body breakup [19]. Moreover, observation of a four-body breakup was reported, though it was not a dominant channel [20]. A predissociative model developed by Green and Herbst in an attempt to explain fragmentation of hydrogen containing molecular ions predicts that due to the lightness of hydrogen atoms rupture of H-heavy atom bonds are preferential [8]. However, for some hydrogen containing compounds rupture of heavy atom-heavy atom bonds were observed to be dominant [21–23]. It still remains a challenge to create a model able to predict the fragmentation in the DR reaction.

In a preliminary brief paper we reported an investigation into the DR of the ozone cation [24]. The present paper is an expansion of the earlier published results with more details on the experiment and data analysis. In this paper we report (1) the cross section over an interaction energy region from $\approx$0 to 0.2 eV; (2) the competition between the O_2+O and $O+O+O$ channels; and (3) the dynamics of the three-body fragmentation channel.

II. EXPERIMENT

The experiment was carried out at the heavy-ion storage ring CRYRING, located at the Manne Siegbahn Laboratory, Stockholm, Sweden. A detailed description of the experimental facility is given elsewhere [25], and only a description of relevant parts is given here.

A. Ion source

The beam was made in a Nielsen-type hot filament ion source [26] operated in an untraditional way. The filament was not used, and the source was run in a high voltage glow-discharge mode with the following source parameters. Oxygen was admitted during 8 ms giving a maximum internal source pressure of about 0.3 Torr after a few ms. A voltage of 1.9 kV, via an 810 Ω resistor to the anode, was switched on for 12 ms initiating a discharge and creating a 25 nA beam of O_3^+. The duration of the ion pulse was a few ms, suitable for injection into CRYRING.

B. General description

The ions were extracted from the ion source by a potential of 40 kV, then mass selected by a bending magnet and then injected into the ring. The ions were accelerated to the final beam energy of 1.96 MeV by a radio frequency driven drift tube. The cycle length for this experiment was chosen to be 6 s, which included ion production, injection, acceleration (3 s), internal relaxation of the excited states (0.7 s), data acquisition (1.3 s), and resetting of the ring (1 s). The interaction between the ion beam and a monoenergetic electron beam occurred in a device called the electron cooler placed in one of the straight sections of the ring. The term *electron cooler* derives from the effect of a reduction of the phase space occupied by the ions due to their interaction with the cold electron beam. This effect is most efficient at low interaction energies and for light molecular ions, and it was not observed to be efficient for O_3^+. Due to the acceleration of the electrons in the longitudinal direction from the electron gun cathode and a one hundred times adiabatic expansion of the electron beam, the distribution of the electrons in the ion rest frame is described by the anisotropic Maxwellian distribution with two different temperatures

$$f(v,v_d) = \frac{m_e}{2\pi k T_{e\perp}} \left(\frac{m_e}{2\pi k T_{e\parallel}} \right)^{1/2} \times \exp\left(- \frac{m_e v_\perp^2}{2kT_{e\perp}} - \frac{m_e (v_\parallel - v_d)^2}{2kT_{e\parallel}} \right), \quad (2)$$

where $kT_{e\parallel}$=0.1 meV, $kT_{e\perp}$=2 meV are the longitudinal and transverse electron temperatures, respectively, and v_d is the detuning velocity corresponding to the detuning energy, E_d, given by

$$E_d = \frac{m_e v_d^2}{2} = e(\sqrt{U_{cath}} - \sqrt{U_{cool}})^2, \quad (3)$$

where e is the elementary charge, U_{cath} is the electron cooler cathode voltage which is detuned from the value of U_{cool} corresponding to the case when the average electron and ion velocities are equal. The neutral products of the DR reaction were separated from the ion beam by the dipole magnet located after the electron cooler and continued moving in a straight line where they were detected. For the detection of the DR fragments two principally different kinds of detectors were utilized. An ion-implanted silicon detector (IISD) was used for measuring the DR count rate and branching fractions, while an imaging detector (ID) was used for a detailed investigation of the three-body breakup, viz., final state products and geometries upon dissociation.

C. Ion-implanted silicon detector (energy-sensitive detector)

The IISD was situated at a distance of about 4 m from the middle of the electron cooler. The detector has an active area of 3000 mm^2 and functions as a semiconductor $p-n$ junction. The boron ion-implanted entrance layer is very thin, $\approx$500 Å, and the detection efficiency is 100% for $\approx$MeV particles. A charge-sensitive preamplifier is used before the full amplification of the detector signal. The resolution of the IISD is determined by many factors, the most relevant of which are junction capacitance and leakage current. The resolution of the signal at the present experiment was about 130 keV. The signal from the IISD can be read out either by a multichannel analyzer (MCA) or a multichannel scaler (MCS) via a single-channel analyzer.

D. Imaging detector (position-sensitive detector)

The ID was situated at a distance of about 7 m from the middle of the electron cooler. The ID consists of a stack of three microchannel plates (MCPs), a phosphor screen, and a charge-coupled device (CCD) camera. When a particle hits the first MCP it releases electrons, the number of which increases in a cascade process. The electron cloud after the stack ($\approx 10^8 e$) gives rise to a flash on the phosphor screen which is detected by the CCD camera. The ID operates in a switch-off mode which allows one to read out the CCD frame containing all the fragments originating from the same DR event. Such a mode of operation is accomplished by a fast image intensifier (II) which functions as a shutter of the CCD camera. The first particle arriving from the DR event is detected by a photomultiplier tube. 200 ns later the II is switched off for 2 ms. The delay of 200 ns is long enough for all the particles to reach the ID and 2 ms is required to transfer the data stored in the CCD to the data acquisition computer. A spot-finding routine is used to determine the coordinates of the flashes. A veto signal, which is slightly longer than switch-off time, blocks the system from retriggering on spurious events. The ID operates at a speed of $\approx$300 Hz. The detection efficiency of the ID for a single particle is $\approx$0.6, which is mainly determined by the open area ratio of the MCP.

III. DATA ANALYSIS AND RESULTS

A. Branching fractions

For the DR of O_3^+ at 0 eV collision energy the following channels are energetically allowed (Fig. 1):

$$O_3^+ + e \rightarrow \begin{cases} O_2 + O + 11.43 \text{ eV} & (\alpha) \\ O + O + O + 6.27 \text{ eV} & (\beta) \end{cases}. \tag{4}$$

The quoted energy corresponds to the kinetic energy ($\mathcal{R}_{KE}$) when all of the fragments are formed in their ground states. Since the time difference in reaching the IISD by the DR products is $\approx$ns while the shaping time of the main amplifier is $\approx \mu$s, it is not feasible to detect each fragment individually. As such, the MCA pulse-height spectrum shows only one peak corresponding to the full ion beam energy and it is impossible to determine which channel the fragments originate from. In order to overcome this obstacle, a grid with a known transmission ($t = 0.297 \pm 0.015$) is inserted in front of the IISD [27]. Then the single peak in the MCA spectrum splits into a series of peaks. Each peak corresponds to the total mass of the fragments that passed through the grid (Fig. 2). The background contribution to the pulse-height spectrum originating from collision-induced dissociation reactions with residual gas R_g,

$$O_3^+ + R_g \rightarrow \begin{cases} O_2 + O^+ + R_g, \\ O_2^+ + O + R_g, \\ O^+ + O + O + R_g, \end{cases} \tag{5}$$

and charge-transfer reaction

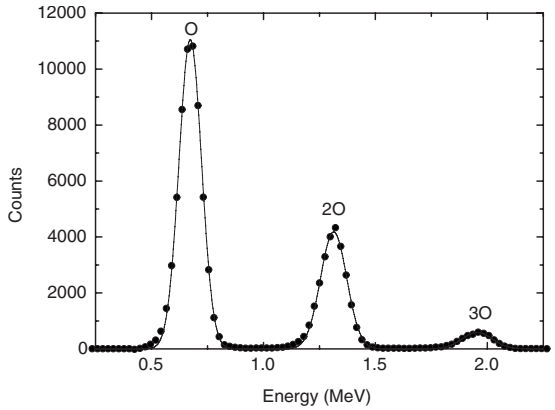

FIG. 2. Background-subtracted pulse-height spectrum recorded with the grid in front of the IISD. The solid lines represent the best Gaussian curves fit to each peak.

$$O_3^+ + R_g \rightarrow \text{neutral fragments} + R_g^+, \tag{6}$$

was taken into account by recording a spectrum at 1 eV interaction energy which was normalized according to the ion current and then subtracted from the initial spectrum. It has been shown that background events dominate the count rate at 1 eV collision energy [28]. The intensity of each peak P_O, P_{2O}, and P_{3O}, can be related to the channel intensities N_α and N_β, through a set of linear equations

$$\begin{bmatrix} P_O \\ P_{2O} \\ P_{3O} \end{bmatrix} = \begin{bmatrix} t(1-t) & 3t(1-t)^2 \\ t(1-t) & 3t^2(1-t) \\ t^2 & t^3 \end{bmatrix} \begin{bmatrix} N_\alpha \\ N_\beta \end{bmatrix}. \tag{7}$$

The branching fractions are calculated after the normalization of the results, and are determined to be

$$n_\alpha = 0.06 \pm 0.03,$$

$$n_\beta = 0.94 \pm 0.03. \tag{8}$$

The errors mostly originate from uncertainty in the grid transmission.

B. Cross section and rate coefficient

The cathode voltage ramp method was used to vary the detuning energy from $\approx$0 eV up to 1 eV. The voltage was linearly changed from 36.3 to 16.2 V, which covered this interaction energy range twice; once when the electrons were faster than the ions and vice versa. The counts of the DR events within a dwell time of 2 ms were measured by an MCS in combination with the IISD. The DR rate coefficient $\alpha(E_d)$, is related to the count rate dN/dt, as

$$\alpha(E_d) = \frac{dN}{dt} \frac{v_e v_i e^2}{I_e I_i} \frac{\pi r_e^2}{l}, \tag{9}$$

where v_e and v_i are the electron and ion velocities, respectively, I_e and I_i are the electron and ion currents, respectively, r_e is the electron beam radius, and l is the interaction region length. However, since the count rate at 1 eV was dominated

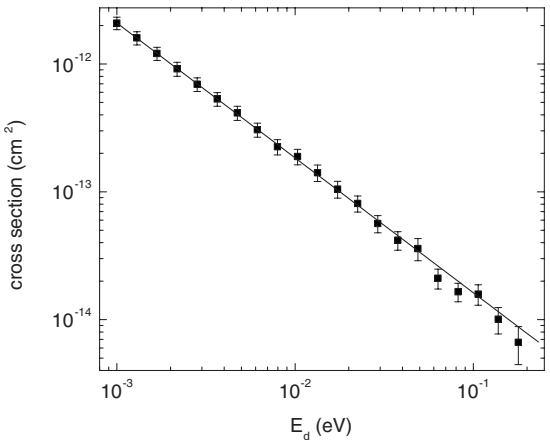

FIG. 3. Measured cross section versus detuning energy with statistical error bars. The solid line shows the best fit [Eq. (10)].

by charge-transfer reactions with the residual gas [Eq. (6)], this value was used as the background contribution and was subtracted from the count rate at every point of the interaction energy scan enabling one to obtain a pure DR MCS spectrum. Due to the velocity spread of the electrons in the electron cooler the rate coefficient is a velocity weighted cross section averaged over the distribution presented in Eq. (2). At collision energies where the electron velocity spread is negligible, the detuning energy equals the center-of-mass (c.m.) energy and the cross section can be obtained by division of the rate coefficient by the detuning velocity (Fig. 3). The obtained result was corrected for toroidal regions of the electron cooler and the space-charge effect induced by the electrons [29,30].

The thermal rate coefficient can be found by folding the velocity weighted cross section with an isotropic Maxwellian distribution. Assuming that the cross section is given by

$$\sigma(E) = \frac{1.43 \times 10^{-15}}{E(eV)^{1.05}} \ \text{cm}^2, \tag{10}$$

then the thermal rate coefficient can be expressed in the following way:

$$\alpha(T) = 1.43 \times 10^{-15} e^{1.05} \sqrt{\frac{8}{\pi m_e}} \Gamma(0.95)(kT)^{-0.55} \ \text{cm}^3 \ \text{s}^{-1}, \tag{11}$$

where Γ is the gamma function. Taking into account the statistical uncertainties in the cross section (Fig. 3) the thermal rate coefficient can be written as

$$\alpha(T) = (7.37 \pm 1.08) \times 10^{-7} \left(\frac{T}{300}\right)^{-0.55 \pm 0.01} \ \text{cm}^3 \ \text{s}^{-1}. \tag{12}$$

The systematic uncertainty in the value can be as high as 15% and mostly originates from the uncertainties in the electron cooler length, the electron and ion beam currents.

C. Imaging data analysis

1. Final state products

In the three-body fragmentation channel, the atomic fragments can be formed in the following combinations of states (Fig. 1):

$$O_3^+ + e^- \rightarrow \begin{cases} O(^3P) + O(^3P) + O(^3P) + 6.27 \ \text{eV} & (\beta_1) \\ O(^3P) + O(^3P) + O(^1D) + 4.30 \ \text{eV} & (\beta_2) \\ O(^3P) + O(^1D) + O(^1D) + 2.33 \ \text{eV} & (\beta_3) \\ O(^3P) + O(^3P) + O(^1S) + 2.08 \ \text{eV} & (\beta_4) \\ O(^1D) + O(^1D) + O(^1D) + 0.36 \ \text{eV} & (\beta_5) \\ O(^3P) + O(^1D) + O(^1S) + 0.11 \ \text{eV} & (\beta_6) \end{cases}. \tag{13}$$

The higher the excitation of the DR products, the less kinetic energy is available, which results in a smaller separation between the fragments on the imaging detector. For each CCD frame the transverse fragment displacements from the c.m. $d_{O_i-\text{cm}}$, were calculated. The total kinetic energy released in the detector plane is proportional to the total displacement ($\mathcal{D}_{\text{tot}}$) value that is related to $d_{O_i-\text{cm}}$ values as

$$\mathcal{D}_{\text{tot}} = \sqrt{\sum d^2_{O_i-\text{cm}}}. \tag{14}$$

However, due to the random orientation of the molecular plane with respect to the MCP surface, for the individual channel the $\mathcal{D}_{\text{tot}}$ varies from 0 up to the maximum value proportional to the $\mathcal{R}_{\text{KE}}$. Analytical expressions for the $\mathcal{D}_{\text{tot}}$ distribution are known only for two-body breakup [31]. The Monte Carlo simulation developed by Müller and Cosby for homonuclear three-body breakup was used to calculate such distribution [32]. Due to the momentum and energy conservation law restrictions, the velocity vectors of the oxygen atoms can be determined by five independent parameters. In the Monte Carlo simulation three of them are Eulerian angles, which orientate the molecular plane in the space, and other two are fractions of the $\mathcal{R}_{\text{KE}}$ received by two of the fragments. Since at $\approx$0 eV interaction energy all possible directions are equally probable, i.e., an isotropic distribution, the Eulerian angles can be assumed to be uniformly distributed. The resulting Monte Carlo $\mathcal{D}_{\text{tot}}$ distributions for randomly distributed parameters are shown in Fig. 4. The Monte Carlo $\mathcal{D}_{\text{tot}}$ distributions of each channel were scaled to the experimental data and normalized scaling parameters determined branching fractions of the final state products (Table I).

2. Molecular geometries upon dissociation

In order to investigate the molecular geometries upon dissociation the Dalitz plot method is used in which coordinates η_1 and η_2 are calculated as

$$\eta_1 = (2E_3 - E_2 - E_1)/(3\mathcal{R}_{\text{KE}}),$$

$$\eta_2 = (E_2 - E_1)/(\sqrt{3}\mathcal{R}_{\text{KE}}), \tag{15}$$

where E_i is the fragment energy [33]. Note that each point on the Dalitz plot represents unique dissociation geometry. The

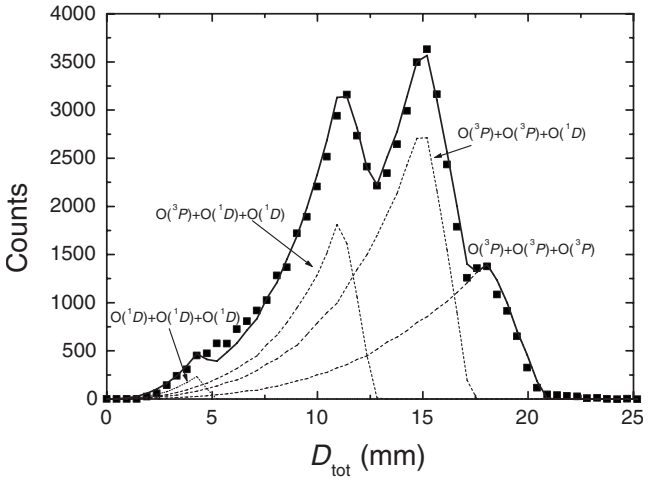

FIG. 4. Experimentally measured $\mathcal{D}_{tot}$ distribution of all three-body events is shown by the solid squares. The Monte Carlo simulation distributions for four populated channels are depicted by the dashed lines. The solid line represents the best fit of the Monte Carlo distributions to experimental data.

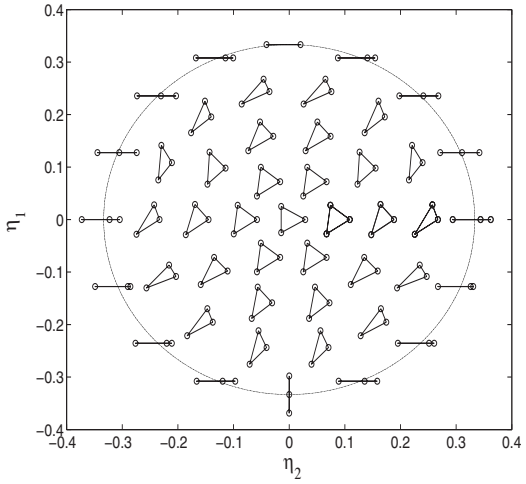

FIG. 5. The relation between Dalitz coordinates and geometries upon dissociation.

relation between molecular dissociation geometries and Dalitz coordinates is shown in Fig. 5. Since the ID was used only to collect two-dimensional data, only the transverse projection of the oxygen atom momenta on the MCP surface could be measured. The transverse Dalitz coordinates (Q_1, Q_2) cannot describe the dissociation geometries since each transverse projection can originate from a variety of geometries in the molecular plane and only the transverse Dalitz coordinates when $Q_1=0$ and $Q_2=0$ contain information solely about the equilateral breakup. For instance, each dissociation geometry contributes to the transverse linear geometries such that linear breakup is overestimated in the transverse plane. It can be clearly seen from the transverse Dalitz distribution obtained from the Monte Carlo simulation plotted for the case when all breakup geometries are equally probable [Fig. 6(a)]. The straightforward method to extract information about dissociation geometries in the molecular plane is to divide the experimental transverse Dalitz distribution with the distribution presented in Fig. 6(a). The validity of such a *weighting* procedure clearly indicating the preferred or nonpreferred dissociation geometries was shown in Ref. [34]. For the three-body channel when all particles are formed in the ground states (β_1) the transverse Dalitz distribution was plotted for events with $\mathcal{D}_{tot} > 18.5$ mm in order to avoid contamination by the β_2 channel (Fig. 4). Using the *weighting* procedure, the dissociation geometries for the β_1 channel are shown in Fig. 6(b). It would be, in particular, interesting to investigate the breakup geometries for the different populated three-body channels. Since the Dalitz plot is known for the β_1 channel [Fig. 6(b)], its contribution can be suppressed for the events with $\mathcal{D}_{tot}$ from 14 to 16 mm enabling the construction of the Dalitz plot originating predominantly from the β_2 channel [Fig. 6(c)]. Using the same technique the Dalitz plot can also be obtained for the β_3 channel regarding the events with $\mathcal{D}_{tot}$ from 7.5 to 11.5 mm [Fig. 6(d)].

IV. DISCUSSION

DR can proceed via two different routes: the so-called direct and indirect mechanisms [35,36]. In the direct mechanism the electron is directly captured to the doubly excited neutral intermediate state which then dissociates, while the indirect mechanism involves vibrationally excited predissociative Rydberg states. Both mechanisms are resonant processes, though due to the nuclear motion the direct mechanism can occur over a wide range of interaction energies. The cross section of DR proceeding via the direct mechanism is inversely proportional to the interaction energy [37]. The cross section measured for the DR of O_3^+ up to 0.2 eV closely follows the characteristics of the direct mechanism. It would also be instructive to compare the DR rate coefficient for different oxygen containing ions. An experiment carried out using the stationary afterglow technique showed that the rate coefficient for the molecular oxygen dimer $O_2 \cdot O_2^+$, was 42×10^{-7} cm^3 s^{-1} [38]. Such an unusually high rate coefficient was referred to as a superdissociative recombination [39]. CRYRING experiments showed the rate coefficients for O_3^+ of 7.37×10^{-7} cm^3 s^{-1} [Eq. (12)] and for O_2^+ of 2.4×10^{-7} cm^3 s^{-1} [40]. It seems that the more complex the

TABLE I. Calculated values of the electronic branching fractions of the available three-body fragmentation channels. The quoted error bars originate from both the statistical uncertainties of the individual channel intensities and the uncertainty in conversion from CCD camera pixel size to mm.

Channel	β_1	β_2	β_3	β_4	β_5	β_6
Fraction	0.28 ± 0.03	0.50 ± 0.03	0.21 ± 0.02	0 ± 0.01	0.01 ± 0.05	0 ± 0.01

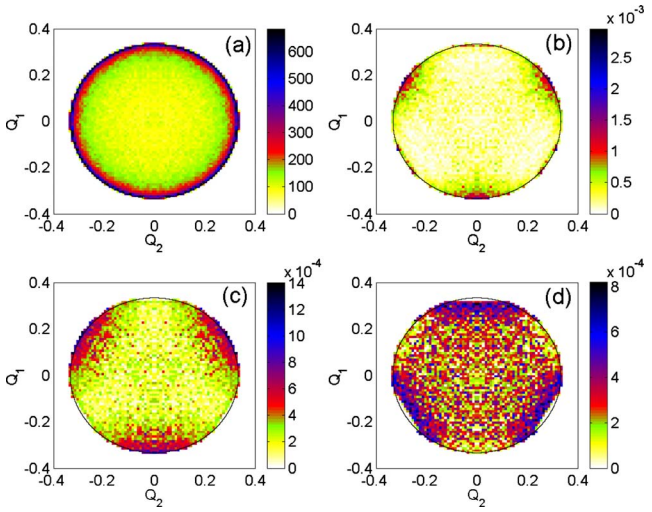

FIG. 6. (Color online) Monte Carlo simulated transverse Dalitz distribution when all breakup geometries are equally probable in the molecular plane (a). The preferred geometries upon breakup for the β_1,β_2,β_3 channels [(b),(c),(d)].

molecular structure, the more efficient the DR, which might be correlated with the higher number of states available to participate in the DR process.

A strong propensity to dissociate into the three-body channel was observed. It is noted that the DR rate coefficient is well established to be about 10^{-7} cm^3 s^{-1} at room temperature, while the fragmentation is not completely understood. Few attempts have been made to create models capable of predicting branching fractions [7–11]. In 1978 Herbst introduced a statistical model [7]. In this approach, the probability of a certain channel is proportional to the number of quantum states existing in the channel, i.e., the more exothermic channels are more probable. This implies that different sets of neutral products are possible with the dominant pathway being single atom loss. Although this model fails to explain the branching fractions reported here, for some cases it agrees with experimental observations [41]. In the valence bond approach created by Bates the probability of the bond rupture is proportional to the charge density surrounding the bond. This assumes that for small polyatomic ions the single bond rupture is dominant, while for more complex ions, in which the charge can be delocalized, a wide assortment of the products is possible [9–11]. This model also fails for the DR of O_3^+, since it predicts that the O_2+O channel must be dominant. It is concluded that such models are not generally valid to explain the DR fragmentation, though they succeeded for individual cases which might be fortuitous. The statistical model developed by Strasser *et al.* [42] gave excellent agreement with experimental observations reported by Datz *et al.* for H_3^+ [12]. It would be, in particular, interesting to extend this model for the triatomic homonuclear ions of O_3^+ and N_3^+ attempting to explain opposite observed fragmentation patterns [43]. However, due to the lack of information about the potential surfaces important for the DR reaction, it is currently not feasible.

It is noted that a DR reaction, which proceeds through the three-body channel with a probability of more than 0.9, has only been observed so far for O_3^+ and $D_5O_2^+$ [18]. For $D_5O_2^+$ the result might be expected since it involves cleavages of the cluster bonds D_2O-D^+-D_2O, while for the ozone cation the result is more unexpected, since the breakup involves the full fragmentation of the valence bonds. For O_3^+ this might be correlated with two factors: (1) the relatively high exothermicity of the three-body channel (6.27 eV) and (2) the availability of many electronically excited three-body channels. The suggestion that the higher surplus energy might enhance the three-body channel was proposed by Vikor *et al.* [44]. The greater the number of product channels which are available means that more intermediate states, after the electron capture, are available which might lead to an enhancement of the three-body channel. Indeed, Herbst's statistical model implies that the probability of a channel is proportional to the number of states existing in the channel [7]. It was also suggested that the primary molecular products originating from the two-body channel are vibrationally and electronically excited, which might then undergo secondary fragmentation also increasing the population of the three-body channel [45]. In order to check the validity of such an assertion the three-body breakup dynamics must be investigated to verify if a sequential mechanism is involved in the DR reaction. Moreover, the high probability to dissociate through the three-body channel for the ozone cation after the capture of a slow electron makes it important to study this channel in more detail.

A variety of studies have been devoted to the photodissociation of ozone by uv solar radiation ranging from 240 to 290 nm (see, for instance, Ref. [46]), though only a few have been carried out at higher photon energies [47,48]. A similar tendency for three-body breakup could be observed in the photodissociation of the neutral ozone molecule at photon energies close to the ionization energy. In this case, the potential energy surfaces, which are involved in the DR reaction, might also play a role in the photodissociation process. Indeed, if the photon wavelength is 193 nm, which lies 0.16 eV above the $O(^3P)+O(^3P)+O(^3P)$ limit, the three-body breakup channel constitutes 2% of the total reactivity [49]. However, when the photon energy was raised to 7.86 eV (157.6 nm) three-body fragmentation was observed to be comparable to two-body breakup [50]. Moreover, similarities in the dynamics of the photodissociation and DR reactions were also found for the SD_2 molecule [28].

In the DR of the ozone cation, six three-body channels are energetically available [Eq. (13)]. The Monte Carlo simulation fit to the data showed that only three of them are significantly populated $(\beta_1,\beta_2,\beta_3)$. The production of atomic oxygen in the second excited state (^1S) is unfavored in both the β_4 and β_6 channels. Due to the importance of this state for the green aurora and airglow, many studies have been carried out to investigate the ^1S quantum yield from the DR of the ionized oxygen molecule. As measured at CRYRING, the branching fraction for the $O(^1S)+O(^1D)$ channel at low collision energy was about 5% [40], which agrees with predictions from the spin-orbit coupling model of Guberman [51]. From the DR of NO^+ and CO^+, channels producing $O(^1S)$ are endothermic at 0 eV collision energy. In order to reach these limits the interaction energy was raised to 5.6

and 1.5 eV, respectively. This resulted in the appearance of the $N(^2D)+O(^1S)$ channel with a relative intensity of 10% [52], while the $C(^3P)+O(^1S)$ channel was not observed [53]. The unfavorable formation of atomic oxygen in the ^1S state might be a general tendency in the DR of oxygen containing compounds. This might be related to the minimal electronic degeneracy of the ^1S state compared to the other oxygen states. Indeed, purely statistical approaches sometimes correctly predict the observed electronic branching fractions [52,54]. However, such models fail for the present study since they predict the channel β_1 to be dominant.

The Dalitz plot for the β_1 channel [Fig. 6(b)] shows that the favored geometries for the three-body breakup are those which are close to linear. It is noted that a very similar preference was observed for H_3^+ [34]. The observed dissociation geometries suggest that the reaction proceeding through the β_1 channel is not an instantaneous process, otherwise the molecular ion geometry ($r_0=1.25$ Å, $\theta=131.5°$ [55]) would dominate in the Dalitz plot. Therefore, there must be sufficient time after the electron capture for a rearrangement in the molecular geometry. The $\mathcal{R}_{KE}$ is most likely shared in such a way that the central atom receives only a minute fraction of the energy and the rest is almost equally distributed between the other two oxygen atoms. Such a $\mathcal{R}_{KE}$ distribution corresponds to the case when the breakup proceeds via a synchronous concerted mechanism in which the two O-O bonds break simultaneously. It is worth noting that in the dissociation of the neutral ozone molecule initiated by 193 nm photon excitation the $O(^3P)+O(^3P)+O(^3P)$ breakup proceeds through an almost linear geometry via a synchronous fragmentation process [49]. A preference to dissociate at a linear open geometry was observed for all triatomic molecular ions studied so far [14,16,28,34,54]. The Dalitz plot for the β_2 channel [Fig. 6(c)] reveals similar dynamics to the β_1 channel. A different Dalitz plot was obtained for the β_3 channel [Fig. 6(d)]. There are three equal groups of preferred breakup geometries [Fig. 6(d)] due to the symmetry of the Dalitz coordinates through interchange of the fragments (Fig. 5). For simplicity, we consider one of them along $Q_1 \approx 0.3$, which indicates that one of the atoms receives the same amount of $\mathcal{R}_{KE}$ ($\approx 60\%$) and the rest is broadly shared between the two other oxygen fragments. This might be evidence for a sequential breakup, i.e., upon the first bond cleavage the free oxygen atom receives $\approx 60\%$ of the available $\mathcal{R}_{KE}$ and the remaining O_2 molecule stays intact for a time longer than a rotational period, which makes the second bond rupture independent from the first. Due to the rotational motion of the O_2 molecule the second bond cleavage involves more random energy sharing [56]. Evidence for such a sequential breakup mechanism was reported for the DR of SD_2^+ [28].

V. CONCLUSIONS

A detailed investigation into the DR reaction of the ozone cation has been performed at the storage ring CRYRING. The obtained rate coefficient is similar to those measured for other triatomic molecular ions [43,57–59]. For some more complex ions the rate coefficients were measured to be even higher than 10^{-6} cm^3 s^{-1} [22,23,60], while for diatomic ions it usually does not exceed 3×10^{-7} cm^3 s^{-1} [40,53,61–63]. The increase of the rate coefficient might be related to the enhancement of the internal states relevant for the DR reaction. The analysis of the branching fractions has revealed almost exclusively complete fragmentation of the molecule. Based on experimental observations Vikor *et al.* concluded that population of a three-body channel is proportional to its available energy [44]. The validity of such an assertion is proven for the X_3^+ ions studied so far, i.e., N_3^+—0.08 (0.7 eV), H_3^+—0.77 (4.8 eV), and O_3^+—0.94 (6.27 eV) [12,43]. This suggestion is also valid for XH_2^+ ions, e.g., the full fragmentation channel constitutes 60%–80% for the ions with $\mathcal{R}_{KE}$ of 2.5–4.8 eV [12–16], while for the DR of BH_2^+ it is only 35%, which is then explained by the relatively low $\mathcal{R}_{KE}$ value of 1.56 eV [64]. The three-body breakup channel has been investigated with the imaging detector. In particular, it has been found that the formation of atomic oxygen in the second excited state is highly unfavored. This result is consistent with the DR of other oxygen containing compounds, e.g., CO^+, NO^+, and O_2^+, in which the production of $O(^1S)$ was also observed to be minor [40,52,53]. The breakup dynamics of the $O(^3P)+O(^3P)+O(^3P)$ and $O(^3P)+O(^3P)+O(^1D)$ channels involve a synchronous concerted mechanism, which is similar to the fragmentation of H_3^+ [34]. It would be instructive to investigate the dynamics of the analogous channel in the DR of N_3^+. However, since it constitutes only 8% it is experimentally complicated [43]. The analysis also shows that a sequential mechanism might be involved in the $O(^3P)+O(^1D)+O(^1D)$ breakup. So far theoretical approaches for studying of the DR reaction successfully used for some molecular ions have not been applied for the ozone cation [65]. We encourage such investigation in order to give a more qualified explanation of the reported observations, i.e., overwhelming dominance of the three-body breakup channel and dynamics occurring in this channel.

ACKNOWLEDGMENTS

We would like to thank the staff at the Manne Siegbahn Laboratory for all their assistance during the experiment. This work was supported by the Swedish Research Council, the Swedish National Space Board, and the Swedish Institute.

[1] J. M. Ajello and K. D. Pang, J. Chem. Phys. **61**, 3152 (1974).
[2] P. M. Dehmer and W. A. Chupka, J. Chem. Phys. **62**, 2228 (1975).
[3] D. Smith and P. Spanel, Mass Spectrom. Rev. **14**, 255 (1995).
[4] D. Smith, Chem. Rev. **92**, 1473 (1992).
[5] R. P. Wayne, *Chemistry of Atmospheres* (University Press, Oxford, 2000).
[6] D. Zajfman, Z. Amitay, C. Broude, P. Forck, B. Seidel, M. Grieser, D. Habs, D. Schwalm, and A. Wolf, Phys. Rev. Lett. **75**, 814 (1995).
[7] E. Herbst, Astrophys. J. **222**, 508 (1978).
[8] S. Green and E. Herbst, Astrophys. J. **229**, 121 (1979).
[9] D. R. Bates, Astrophys. J. **306**, L45 (1986).
[10] D. R. Bates, in *Recent Studies in Atomic and Molecular Processes*, edited by A. E. Kingston (Plenum Press, New York, 1987), pp. 1–27.
[11] T. J. Millar, D. J. DeFrees, A. D. McLean, and E. Herbst, Astron. Astrophys. **194**, 250 (1988).
[12] S. Datz, G. Sundström, Ch. Biedermann, L. Broström, H. Danared, S. Mannervik, J. R. Mowat, and M. Larsson, Phys. Rev. Lett. **74**, 896 (1995).
[13] Å. Larson, A. Le Padellec, J. Semaniak, C. Strömholm, M. Larsson, S. Rosén, R. Peverall, H. Danared, N. Djuric, G. H. Dunn, and S. Datz, Astrophys. J. **505**, 459 (1998).
[14] R. D. Thomas, F. Hellberg, A. Neau, S. Rosén, M. Larsson, C. R. Vane, M. E. Bannister, S. Datz, A. Petrignani, and W. J. van der Zande, Phys. Rev. A **71**, 032711 (2005).
[15] S. Rosén, A. Derkatch, J. Semaniak, A. Neau, A. Al Khalili, A. Le Padellec, L. Vikor, R. Thomas, H. Danared M. af Ugglas, and M. Larsson, Faraday Discuss. **115**, 295 (2000).
[16] V. Zhaunerchyk, F. Hellberg, A. Ehlerding, W. D. Geppert, M. Larsson, C. R. Vane, M. E. Bannister, E. M. Bahati, F. Österdahl, M. af Ugglas, and R. D. Thomas, Mol. Phys. **103**, 2735 (2005).
[17] J. Semaniak, Å. Larson, A. Le Padelec, C. Strömholm, M. Larsson, S. Rosén, R. Paverall, H. Danared, N. Djuric, G. H. Dunn, and S. Datz, Astrophys. J. **498**, 886 (1998).
[18] M. B. Någård, J. B. C. Pettersson, A. M. Derkatch, A. Al-Khalili, A. Neau, S. Rosén, M. Larsson, J. Semaniak, H. Danared, A. Kälberg, and M. af Ugglas, J. Chem. Phys. **117**, 5264 (2002).
[19] M. Larsson and R. D. Thomas, Phys. Chem. Chem. Phys. **3**, 4471 (2001).
[20] W. Geppert, A. Ehlerding, F. Hellberg, S. Kalhori, R. D. Thomas, O. Novotny, S. T. Arnold, T. M. Miller, A. A. Viggiano, and M. Larsson, Phys. Rev. Lett. **93**, 153201 (2004).
[21] H. Montaigne, W. D. Geppert, J. Semaniak, F. Österdahl, F. Hellberg, R. D. Thomas, M. af Ugglas, H. Roberts, T. J. Millar, V. Zhaunerchyk, M. Kaminska, A. Al-Khalili, A. Källberg, and M. Larsson, Astrophys. J. **631**, 653 (2005).
[22] W. D. Geppert, R. Thomas, A. Ehlerding, J. Semaniak, F. Österdahl, M. af Ugglas, N. Djuric, A. Paal, and M. Larsson, Faraday Discuss. **127**, 425 (2004).
[23] W. D. Geppert, R. Thomas, F. Hellberg, A. Ehlerding, F. Österdahl, M. af Ugglas, and M. Larsson, Phys. Chem. Chem. Phys. **6**, 3415 (2004).
[24] V. Zhaunerchyk, W. D. Geppert, M. Larsson, R. D. Thomas, E. Bahati, M. E. Bannister, M. R. Fogle, C. R. Vane, and F. Österdahl, Phys. Rev. Lett. **98**, 223201 (2007).
[25] C. Strömholm, J. Semaniak, S. Rosén, H. Danared, S. Datz, W. J. van der Zande, and M. Larsson, Phys. Rev. A **54**, 3086 (1996).
[26] K. O. Nielsen, Nucl. Instrum. **1**, 289 (1957).
[27] A. Neau, A. Al-Khalili, S. Rosén, A. Le Padellec, A. M. Derkatch, W. Shi, L. Vikor, M. Larsson, J. Semaniak, R. Thomas, M. B. Någård, K. Andersson, H. Danared, and M. af Ugglas, J. Chem. Phys. **113**, 1762 (2000).
[28] F. Hellberg, V. Zhaunerchyk, A. Ehlerding, W. D. Geppert, M. Larsson, R. D. Thomas, M. E. Bannister, E. Bahati, C. R. Vane, F. Österdahl, P. Hlavenka, and M. af Ugglas, J. Chem. Phys. **122**, 224314 (2005).
[29] D. R. DeWitt, R. Schuch, H. Gao, W. Zong, S. Asp, C. Biedermann, M. H. Chen, and N. R. Badnell, Phys. Rev. A **53**, 2327 (1996).
[30] A. Lampert, A. Wolf, D. Habs, J. Kenntner, G. Kilgus, D. Schwalm, M. S. Pindzola, and N. R. Badnell, Phys. Rev. A **53**, 1413 (1996).
[31] Z. Amitay, D. Zajfman, P. Forck, U. Hechtfischer, B. Seidel, M. Grieser, D. Habs, R. Repnow, D. Schwalm, and A. Wolf, Phys. Rev. A **54**, 4032 (1996).
[32] U. Müller and P. C. Cosby, Phys. Rev. A **59**, 3632 (1999).
[33] R. H. Dalitz, Philos. Mag. **44**, 1068 (1953).
[34] D. Strasser, L. Lammich, H. Kreckel, S. Krohn, M. Lange, A. Naaman, D. Schwalm, A. Wolf, and D. Zajfman, Phys. Rev. A **66**, 032719 (2002).
[35] D. R. Bates, Phys. Rev. **78**, 492 (1950).
[36] J. Bardsley, J. Phys. B **1**, 365 (1968).
[37] E. P. Wigner, Phys. Rev. **73**, 1002 (1948).
[38] J. L. Dulaney, M. A. Biondi, and R. Johnsen, Phys. Rev. A **37**, 2539 (1988).
[39] D. R. Bates, J. Phys. B **25**, 3067 (1992).
[40] R. Peverall, S. Rosén, J. R. Peterson, M. Larsson, A. Al-Khalili, L. Vikor, J. Semaniak, R. Bobbenkamp, A. Le Padellec, A. N. Maurellis, and W. J. van der Zande, J. Chem. Phys. **114**, 6679 (2001).
[41] J. Semaniak, B. F. Minaev, A. M. Derkatch, F. Hellberg, A. Neau, S. Rosén, R. Thomas, M. Larsson, H. Danared, A. Paal, and M. af Ugglas, Astrophys. J., Suppl. Ser. **135**, 275 (2001).
[42] D. Strasser, J. Levin, H. B. Pedersen, O. Heber, A. Wolf, D. Schwalm, and D. Zajfman, Phys. Rev. A **65**, 010702(R) (2001).
[43] V. Zhaunerchyk, W. D. Geppert, E. Vigren, M. Hamberg, M. Danielsson, M. Larsson, R. D. Thomas, M. Kaminska, and F. Österdahl, J. Chem. Phys. **127**, 014305 (2007).
[44] L. Vikor, A. Al-Khalili, H. Danared, N. Djuric, G. H. Dunn, M. Larsson, A. Le Padellec, S. Rosén, and M. af Ugglas, Astron. Astrophys. **344**, 1027 (1999).
[45] E. Herbst and H. H. Lee, Astrophys. J. **485**, 689 (1997).
[46] E. Baloitcha and G. G. Balint-Kurti, Phys. Chem. Chem. Phys. **7**, 3829 (2005).
[47] T. Gejo, K. Okada, T. Ibuki, and N. Saito, J. Phys. Chem. **103**, 4598 (1999).
[48] L. Rosenqvist, K. Wiesner, A. N. de Brito, M. Bässler, R. Feifel, I. Hjelte, C. Miron, H. Wang, M. N. Piancastelli, S. Svensson, O. Björneholm, and S. L. Sorensen, J. Chem. Phys. **115**, 3614 (2001).
[49] D. Stranges, X. Yang, J. D. Chesko, and A. G. Suits, J. Chem. Phys. **102**, 6067 (1995).
[50] M. R. Taherian and T. G. Slanger, J. Chem. Phys. **83**, 6246 (1985).

[51] S. L. Guberman, Science **278**, 1276 (1997).
[52] F. Hellberg, S. Rosén, R. Thomas, A. Neau, M. Larsson, A. Petrignani, and W. J. van der Zande, J. Chem. Phys. **118**, 6250 (2003).
[53] S. Rosén, R. Peverall, M. Larsson, A. Le Padellec, J. Semaniak, Å. Larson, C. Strömholm, W. J. van der Zande, H. Danared, and G. H. Dunn, Phys. Rev. A **57**, 4462 (1998).
[54] R. Thomas, S. Rosén, F. Hellberg, A. M. Derkatch, M. Larsson, S. Datz, R. Dixon, and W. J. van der Zande, Phys. Rev. A **66**, 032715 (2002).
[55] S. Willitsch, F. Innocenti, J. M. Dyke, and F. Merkt, J. Chem. Phys. **122**, 024311 (2005).
[56] A. Hishikawa, H. Hasegawa, and K. Yamanouchi, Chem. Phys. Lett. **361**, 245 (2002).
[57] A. A. Viggiano, A. Ehlerding, F. Hellberg, R. D. Thomas, V. Zhaunerchyk, W. D. Geppert, H. Montaigne, M. Larsson, M. Kaminska, and F. Österdahl, J. Chem. Phys. **122**, 226101 (2005).
[58] M. Hamberg, W. D. Geppert, S. Rosén, F. Hellberg, A. Ehlerding, V. Zhaunerchyk, M. Kaminska, R. D. Thomas, M. af Ugglas, A. Källberg, A. Simonsson, A. Paal, and M. Larsson, Phys. Chem. Chem. Phys. **7**, 1664 (2005).
[59] W. D. Geppert, F. Hellberg, A. Ehlerding, J. Semaniak, F. Österdahl, M. Kaminska, V. Zhaunerchyk, A. Al-Khalili, M. af Ugglas, R. Thomas, A. Källberg, and M. Larsson, Astrophys. J. **610**, 1228 (2004).
[60] W. D. Geppert, A. Ehlerding, F. Hellberg, J. Semaniak, F. Österdahl, M. Kaminska, A. Al-Khalili, V. Zhaunerchyk, R. Thomas, M. af Ugglas, A. Källberg, A. Simonsson, and M. Larsson, Astrophys. J. **613**, 1302 (2004).
[61] O. Novotny, J. B. A. Mitchell, J. L. LeGarrec, A. I. Florescu-Mitchell, C. Rebrion-Rowe, A. Svendsen, M. A. El Ghazaly, L. H. Andersen, A. Ehlerding, A. A. Viggiano, F. Hellberg, R. D. Thomas, V. Zhaunerchyk, W. D. Geppert, H. Montaigne, M. Kaminska, F. Österdahl, and M. Larsson, J. Phys. B **38**, 1471 (2005).
[62] J. R. Peterson, A. Le Padellec, H. Danared, G. H. Dunn, M. Larsson, Å. Larson, R. Peverall, C. Strömholm, S. Rosén, M. af Ugglas, and W. J. van der Zande, J. Chem. Phys. **108**, 1978 (1998).
[63] A. Petrignani, W. J. van der Zande, P. C. Cosby, F. Hellberg, R. D. Thomas, and M. Larsson, J. Chem. Phys. **122**, 014302 (2005).
[64] V. Zhaunerchyk (unpublished).
[65] V. Kokoouline and C. H. Greene, Phys. Rev. A **68**, 012703 (2003).